

Supplemental Information

Changes in PM_{2.5} Peat Combustion Source Profiles with Atmospheric Aging in an Oxidation Flow Reactor

Judith C. Chow^{1,2*}, Junji Cao^{2,3}, L.-W. Antony Chen⁴, Xiaoliang Wang¹, Qiyuan Wang^{2,3}, Jie Tian^{2,3}, Steven Sai Hang Ho^{1,5}, Adam C. Watts¹, Tessa B. Carlson¹, Steven D. Kohl¹, John G. Watson^{1,2}

¹Division of Atmospheric Sciences, Desert Research Institute, Reno, Nevada, USA

²Key Laboratory of Aerosol Chemistry and Physics, Institute of Earth Environment, Chinese Academy of Sciences, Xi'an, 710061, China.

³CAS Center for Excellence in Quaternary Science and Global Change, Xi'an, 710061, China

⁴Department of Environmental and Occupational Health, University of Nevada, Las Vegas, Nevada, USA

⁵Hong Kong Premium Services and Research Laboratory, Hong Kong, China

Revised and resubmitted to
Atmospheric Measurement Techniques Discussion

Date

19 August 2019

*Corresponding Author: judith.chow@dri.edu

S.1 Experimental Details and Oxidation Flow Reactor Operation

Oxidation Flow Reactors (OFRs) intend to simulate photochemical changes in gas and particle mixtures as they age during atmospheric transport. This is accomplished by directing fresh emissions through a chamber that is illuminated with ultraviolet (UV) light to simulate the Sun's illumination of the mixture. OFRs differ from smog chambers in that the UV radiation is more intense and there is a continuous flow through the system, rather than the stagnant mixture that is examined in the smog chamber at UV levels closer to ambient levels (Hidy, 2019; Lee et al., 2009). Various OFR systems have been developed and applied (Aerodyne, 2019; Bin Babar et al., 2017; Cazorla and Brune, 2010; Ezell et al., 2010; Huang et al., 2017; Karjalainen et al., 2016; Lambe et al., 2011; Mitroo et al., 2018; Pourkhesalian et al., 2015; Reece et al., 2017; Smith et al., 2009) since the original Teflon bag of Kang et al. (2007) that was externally illuminated with mercury vapor lamps. These units range in volume from 0.15 L (Keller and Burtscher, 2012) to 1200 L (Ezell et al., 2010) and are made from fluorinated ethylene propylene (FEP) Teflon films, stainless steel, quartz or Iridite/Anodine coated aluminum with the intent to minimize reactions with the chamber walls. Although many published articles reference the characterization and operational details of Kang et al. (2007), it is evident that there have been many changes since their initial development.

Important OFR design parameters are (Huang et al., 2017): 1) gas introduction mixing prior to and within the OFR chamber; 2) chamber volume and range of flow rates that determine residence time within the chamber; 3) reaction chamber materials that minimize artifacts (e.g., reactant adsorption and outgassing); and 4) sensors applied to detect the types of reactants and end-products. General findings are: 1) larger diameters and shorter residence times minimize gas and particle losses to chamber surfaces; 2) rapid mixing of pollutants provides more accurate reaction rate measurements; and 3) passivated conductive surfaces minimize electrostatic effects on particles. Although the Caltech Photooxidation Flow Tube reactor (Huang et al., 2017) appears to be the best characterized via modeling and experiment, the Aerodyne (2019) potential aerosol mass (PAM)-OFR is in more widespread use owing to its compactness, reliability, expanding user-base (PAMWiki, 2019), and commercial availability. The Aerodyne OFR was used for the experiments reported here.

Figure S1 illustrates the configuration for these experiments. Two tubular low-pressure mercury (Hg) lamps in the OFR with Teflon sleeves provided UV light at 185 and 254 nm wavelengths (BHK, 2019) and two lamps with doped quartz sleeves provided illumination at 254 nm. Lamps were cooled by a continuous flow of relatively inert, nitrogen (N₂) gas. The main reactions for this OFR185 mode that create O₃, OH (hydroxyl radical), and HO₂ (hydroperoxyl radical) oxidants are:



The OH is most influential in photochemical aging, and OH production within the OFR is related to the Hg lamp intensity, which in turn is related to the voltages applied to the lamps.

Bhattacharai et al. (2018) demonstrate that UV fluxes are almost linearly associated with lamp voltage from 2 to 7 V, and similar linear results were found for the profile aging tests reported here (Cao et al., 2019). OH production is related to lamp intensity by inference from first order reactions of OH with SO₂ which has a well-characterized rate constant ($k_{\text{SO}_2, \text{OH}} = 9.49 \times 10^{-13} \text{ cm}^3 \text{ molecule}^{-1} \text{ sec}^{-1}$ at 1 atm and 298 °K) (Davis et al., 1979; Sander et al., 2006) by the relationship:

$$\text{OH} = -1/k_{\text{SO}_2, \text{OH}} \ln (\text{C}_{\text{SO}_2, \text{out}}/\text{C}_{\text{SO}_2, \text{in}}) \quad (7)$$

where

$k_{\text{SO}_2, \text{OH}}$ = reaction rate of SO₂ with OH ($\text{cm}^3 \text{ molecule}^{-1} \text{ sec}^{-1}$)

$\text{C}_{\text{SO}_2, \text{in}}$ = SO₂ concentration injected into the OFR (ppb)

$\text{C}_{\text{SO}_2, \text{out}}$ = SO₂ concentration at the OFR outlet (ppb)

UV lamps were operated at 2 and 3.5 volts with a flow rate of 10 L min⁻¹ and a plug-flow residence time of ~80 s in the 13.3 L anodine-coated reactor, which translates to OH exposures (OH_{exp}) of $\sim 2.6 \times 10^{11}$ and 8.8×10^{11} molecules-sec cm⁻³ at 2 volts and 3.5 volts, respectively. These values for OH_{exp} are within the range of 1×10^{10} to $\sim 2 \times 10^{12}$ molecules-sec cm⁻³ reported in other OFR experiments. The lamps were powered and brought into steady state operations before drawing the sample stream through the OFR

The Aerodyne OFR surface-to-volume ratio is 0.24 cm⁻¹, which is larger than many of the other OFR types and is intended to minimize particle and gas losses with lamp off. SO₂ concentrations measured ranging from 100 to 800 ppb at the OFR inlet showed less than 1% changes when measured at the OFR outlet. Similar results were found for carbon monoxide (CO) and ozone (O₃), indicating minimal losses to the reactor surfaces. This is in contrast to the Teflon bag of Kang et al. (2007) that experienced SO₂ losses as high as 20%. Lambe et al. (2011) found transmission efficiencies of 0.91 ± 0.09 for CO₂ and 1.2 ± 0.4 for SO₂ with a later quartz glass OFR design.

Lambe et al. (2011) found particle transmission efficiencies exceeding 80% for mobility diameters >150 nm, but as low as 40% for 50 nm particles with a quartz OFR. Karjalainen et al. (2016) measured 60% particle losses for ~20 nm particles, ~25% particle losses for 50 nm particles, and <10% losses for particle sizes >100 nm with a stainless steel OFR. Palm et al. (2016) compared mass concentrations in ambient air within a forest with the same air drawn through an Aerodyne OFR and transfer lines, finding only a 4% particle loss. Bhattacharai et al. (2018) found similar results for ammonium sulfate ((NH₄)₂SO₄) particles, with 50% transmission for 20 nm particles and >90% transmission for particles >100 nm.

For this study, UV lamp stability and linearity was determined by moving a TOCON_C6 photodiode (Sglux GmbH, Germany) detector along the central axis of the OFR and recording its readings as function of the voltage supplied to the lamps, verifying that the UV flux was linearly associated with lamp voltage from 2 to 7 V, but it was undetectable for UV <1.5V and leveled off at ~350 μW cm⁻² in the range of 7-10 V. Experiments were limited to 2 and 3.5 V which is well-within the linear range. Irradiation fluxes were 2.5×10^{13} photons cm⁻² s⁻¹ at 2 V and 12.5×10^{13} photons cm⁻² s⁻¹ at 3.5 V. Fluxes were constant both in time and along the OFR axis, indicating that consistent oxidant amounts can be produced for a given voltage within the linear range, similar

to the findings of Bhattarai et al. (2018). Periodic performance tests of light intensity should be made over time as there may be some deterioration of lamp performance with use, and the measurements need to be repeated when lamps are replaced.

Since high O₃ concentrations were generated when UV lamps were on, a potassium iodide (KI) denuder (1/3 KI with 2/3 silica) was installed at the outlet of the reactor to remove over 99.99% of the O₃ and maintain a stable baseline of < 20 ppb. This possibly compromised some of the potassium ion measurement in the aged profiles.

As discussed in the main text, the biggest uncertainty is not the estimation of oxidant exposure in the OFR, but the conversion of this exposure to atmospheric aging times. Changes in the atmospheric multipollutant environment as emissions from several sources mix in the atmosphere are not represented within the OFR. Added to this are the unknown effects of the high oxidant exposures within the OFR relative to atmospheric exposures and the wide variability of atmospheric OH from the assumed 1.5×10^6 molecules cm⁻³ which is commonly, but not universally, used to translate OH exposure to atmospheric aging.

Supplemental References

- Aerodyne: Potential Aerosol Mass (PAM) oxidation flow reactor, Aerodyne Research Inc., Billerica, MA, 2019. <http://www.aerodyne.com/sites/default/files/u17/PAM%20Potential%20Aerosol%20Mass%20Reactor.pdf>
- Bhattacharai, C., Samburova, V., Sengupta, D., Iaukea-Lum, M., Watts, A. C., Moosmuller, H., and Khlystov, A. Y.: Physical and chemical characterization of aerosol in fresh and aged emissions from open combustion of biomass fuels, *Aerosol Sci. Technol.*, 52, 1266-1282, 2018.
- BHK: Products: Mercury lamps, BHK Inc., Ontario, CA, 2019. <http://www.bhkinc.com/index.cfm?action=products>
- Bin Babar, Z., Park, J. H., and Lim, H. J.: Influence of NH₃ on secondary organic aerosols from the ozonolysis and photooxidation of alpha-pinene in a flow reactor, *Atmos. Environ.*, 164, 71-84, 2017.
- Cao, J. J., Wang, Q. Y., Tan, J., Zhang, Y. G., Wang, W. J., Zhong, B. L., Ho, S. S. H., Chen, L.-W. A., Wang, X. L., Watson, J. G., and Chow, J. C.: Evaluation of the oxidation flow reactor for particulate matter emission limit certification, *Atmos. Environ.*, 2019. submitted, 2019.
- Cazorla, M. and Brune, W. H.: Measurement of ozone production sensor, *Atmos. Meas. Tech.*, 3, 545-555, 2010.
- Davis, D. D., Ravishankara, A. R., and Fischer, S.: SO₂ oxidation via the hydroxyl radical-Atmospheric fate of HSO_x radicals, *Geophysical Research Letters*, 6, 113-116, 1979.
- Ezell, M. J., Johnson, S. N., Yu, Y., Perraud, V., Bruns, E. A., Alexander, M. L., Zelenyuk, A., Dabdub, D., and Finlayson-Pitts, B. J.: A new aerosol flow system for photochemical and thermal studies of tropospheric aerosols, *Aerosol Sci. Technol.*, 44, 329-338, 2010.
- Hidy, G. M.: Atmospheric chemistry in a box or a bag, *Atmosphere*, 10, 1-36, 2019.
- Huang, Y., Coggon, M. M., Zhao, R., Lignell, H., Bauer, M. U., Flagan, R. C., and Seinfeld, J. H.: The Caltech Photooxidation Flow Tube reactor: Design, fluid dynamics and characterization, *Atmos. Meas. Tech.*, 10, 839-867, 2017.
- Kang, E., Root, M. J., Toohey, D. W., and Brune, W. H.: Introducing the concept of Potential Aerosol Mass (PAM), *Atmos. Chem. Phys.*, 7, 5727-5744, 2007.
- Karjalainen, P., Timonen, H., Saukko, E., Kuuluvainen, H., Saarikoski, S., Aakko-Saksa, P., Murtonen, T., Bloss, M., Dal Maso, M., Simonen, P., Ahlberg, E., Svenningsson, B., Brune, W. H., Hillamo, R., Keskinen, J., and Ronkko, T.: Time-resolved characterization of primary particle emissions and secondary particle formation from a modern gasoline passenger car, *Atmos. Chem. Phys.*, 16, 8559-8570, 2016.
- Keller, A. and Bartscher, H.: A continuous photo-oxidation flow reactor for a defined measurement of the SOA formation potential of wood burning emissions, *J. Aerosol Sci.*, 49, 9-20, 2012.
- Lambe, A. T., Ahern, A. T., Williams, L. R., Slowik, J. G., Wong, J. P. S., Abbatt, J. P. D., Brune, W. H., Ng, N. L., Wright, J. P., Croasdale, D. R., Worsnop, D. R., Davidovits, P., and Onasch, T. B.: Characterization of aerosol photooxidation flow reactors: heterogeneous oxidation, secondary organic aerosol formation and cloud condensation nuclei activity measurements, *Atmos. Meas. Tech.*, 4, 445-461, 2011.
- Lee, S. B., Bae, G. N., and Moon, K. C.: Smog chamber measurements. In: *Atmospheric and Biological Environmental Monitoring*, Kim, Y. J., Platt, U., Gu, M. B., and Iwahashi, H. (Eds.), Springer, Dordrecht, Netherlands, 2009.
- Mitroo, D., Sun, Y. J., Combest, D. P., Kumar, P., and Williams, B. J.: Assessing the degree of plug flow in oxidation flow reactors (OFRs): a study on a potential aerosol mass (PAM) reactor, *Atmos. Meas. Tech.*, 11, 1741-1756, 2018.
- PAMWiki: PAMWiki, 2019. <https://sites.google.com/site/pamwiki/>
- Pourkhesalian, A. M., Stevanovic, S., Rahman, M. M., Faghihi, E. M., Bottle, S. E., Masri, A. R., Brown, R. J., and Ristovski, Z. D.: Effect of atmospheric aging on volatility and reactive oxygen species of biodiesel exhaust nanoparticles, *Atmos. Chem. Phys.*, 15, 9099-9108, 2015.
- Reece, S. M., Sinha, A., and Grieshop, A. P.: Primary and photochemically aged aerosol emissions from biomass cookstoves: Chemical and physical characterization, *Environ. Sci. Technol.*, 51, 9379-9390, 2017.
- Sander, S. P., Friedl, R. R., Ravishankara, A. R., Golden, D. M., Kolb, C. E., Kurylo, M. J., Molina, M. J., Moortgat, G. K., Finlayson-Pitts, B. J., Wine, P. H., R.E., H., and Orkin, V. L.: Chemical kinetics and photochemical data for use in atmospheric studies: Evaluation Number 15, Jet Propulsion Laboratory, Pasadena, CA, 2006. https://jpldataeval.jpl.nasa.gov/pdf/JPL_15_AllInOne.pdf
- Smith, J. D., Kroll, J. H., Cappa, C. D., Che, D. L., Liu, C. L., Ahmed, M., Leone, S. R., Worsnop, D. R., and Wilson, K. R.: The heterogeneous reaction of hydroxyl radicals with sub-micron squalane particles: a model system for understanding the oxidative aging of ambient aerosols, *Atmos. Chem. Phys.*, 9, 3209-3222, 2009.

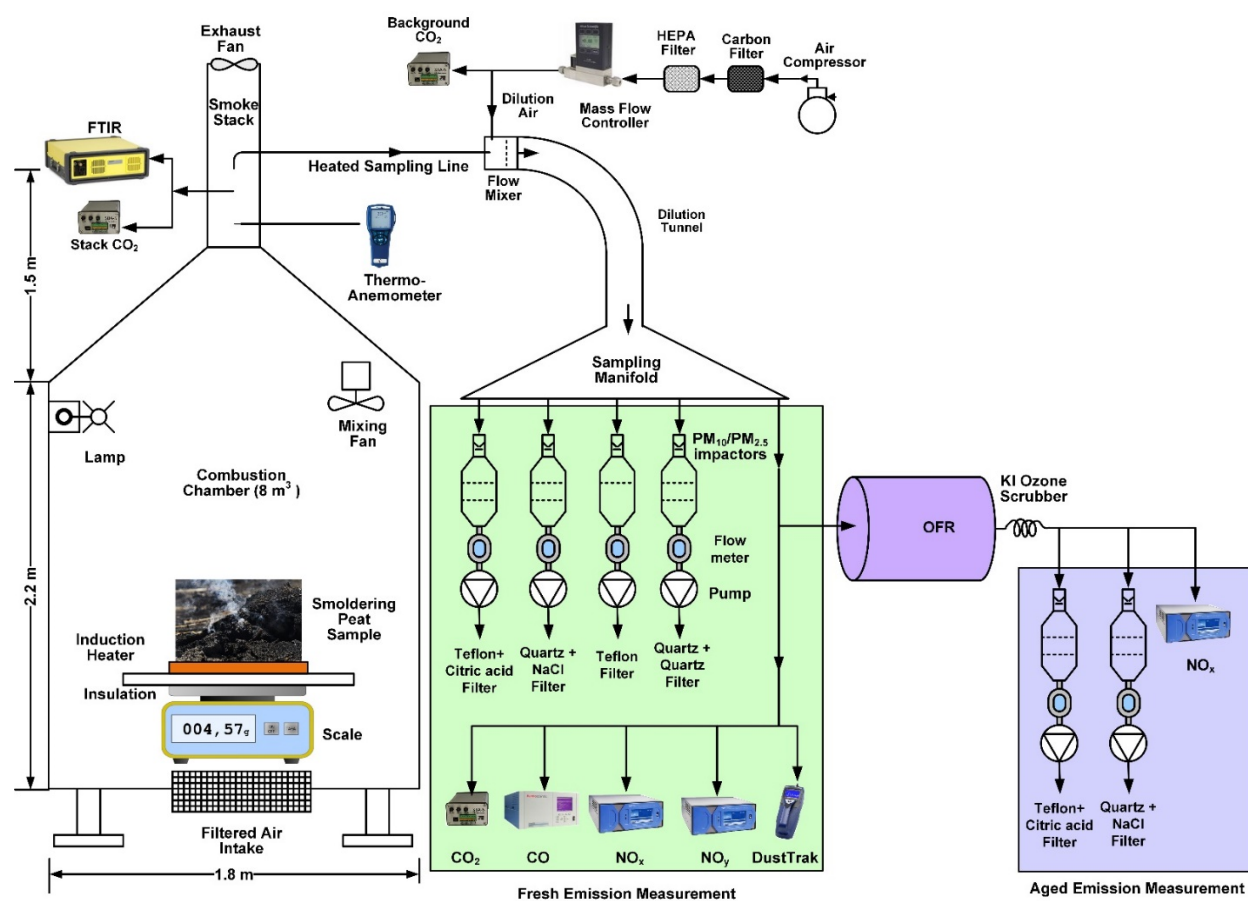


Figure S1. Configuration of peat combustion experimental set up. (FTIR: Fourier-transform infrared spectrometer; OFR: oxidation flow reactor; OFR lamps were operated at 2 and 3.5 volts to simulate aging of ~2 and 7 days, respectively) (Watson et al., 2019).

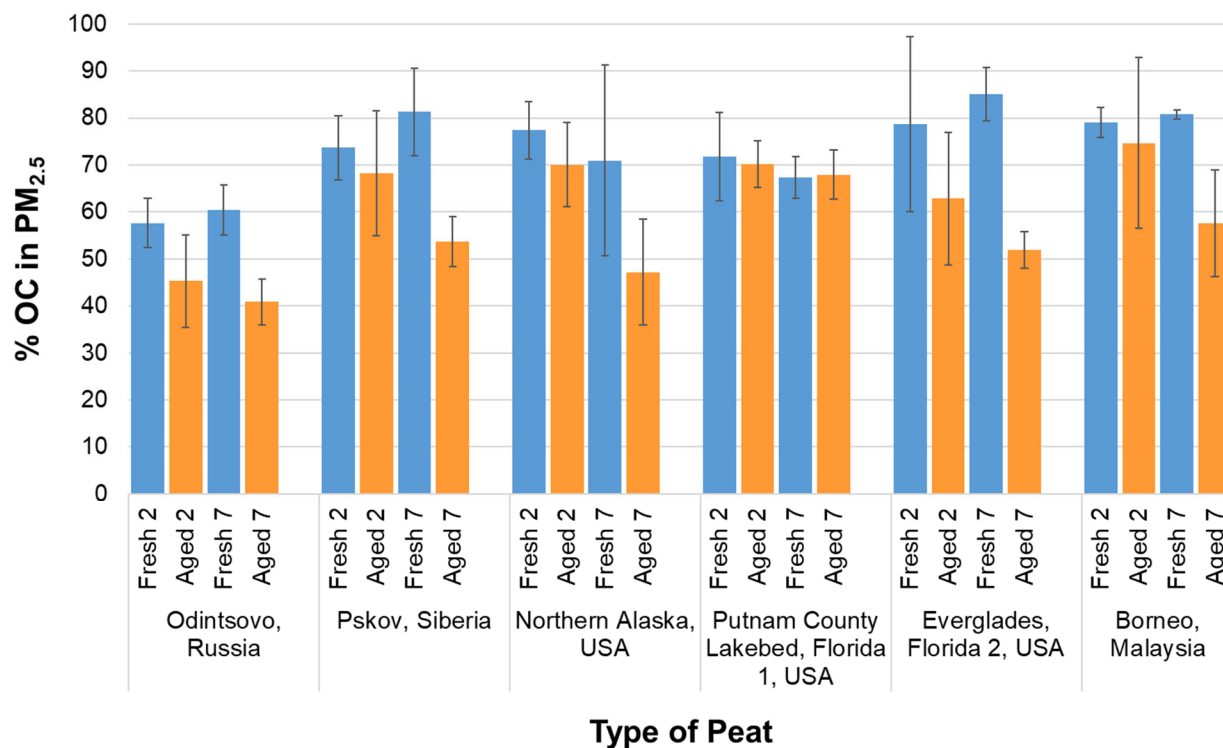
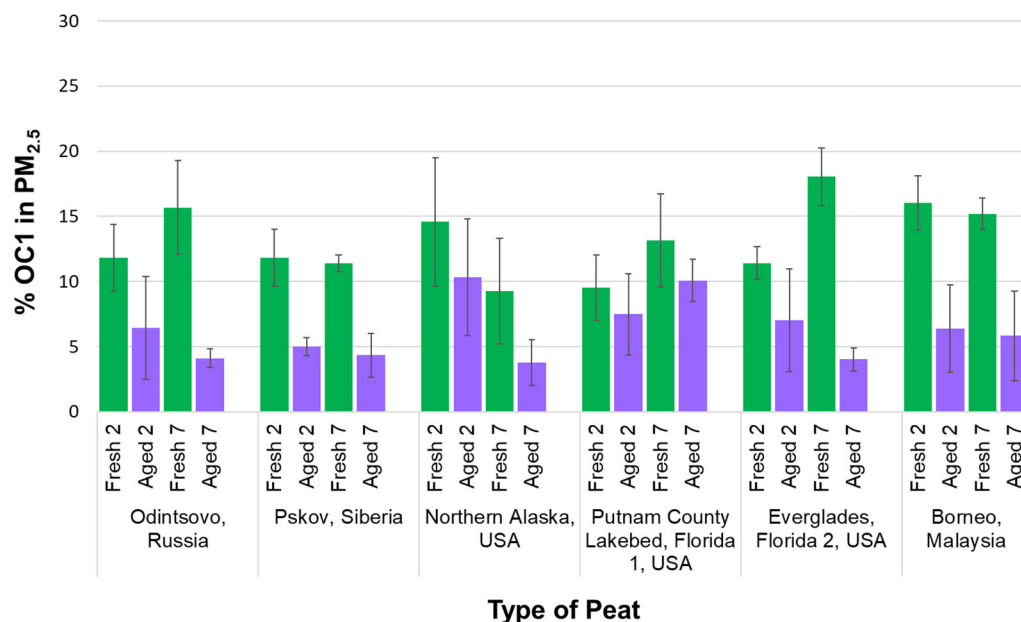


Figure S2. Comparison of OC abundances in PM_{2.5} between the fresh and aged source profiles. Further reduction of OC abundances in PM_{2.5} (~7–22%) from 2- to 7-days of aging are found for all but Putnam (FL1) peat profiles (Fresh 2 vs. Aged 2 and Fresh 7 vs. Aged 7 represent the comparison of 2- and 7-days of atmospheric aging, respectively).

a)



b)

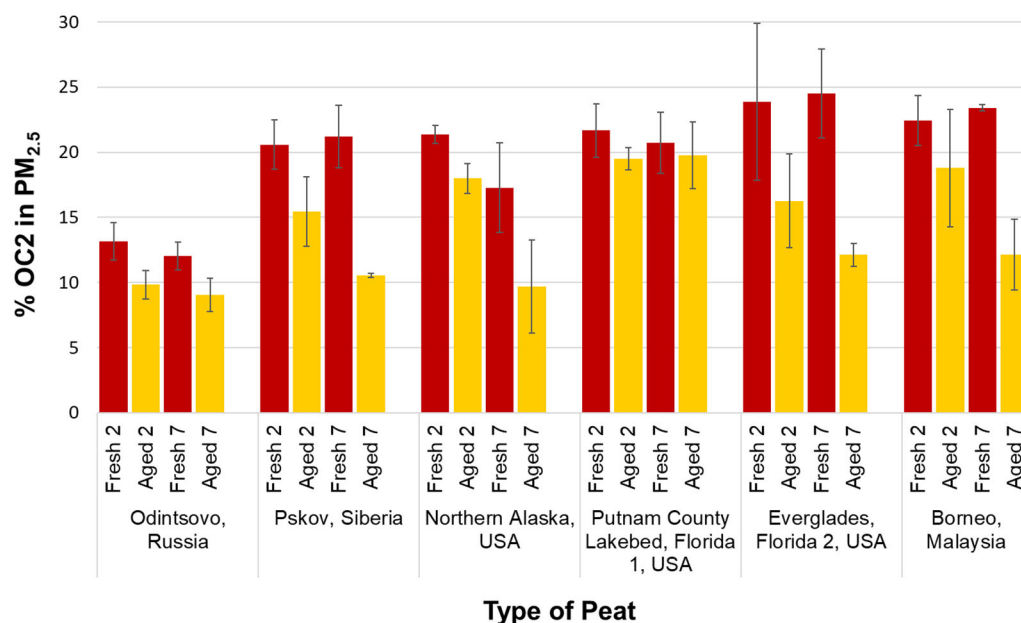


Figure S3. Reduction of low temperature OC1 (a) and OC2 (b) after 2- and 7-days of atmospheric aging. The OC1 and OC2 are carbon fractions thermally evolved at 140 and 280 °C in a helium atmosphere following IMPROVE-A thermal/optical reflectance protocol (Chow et al, 2007) that are applied in U.S. long term IMPROVE network and Chemical Speciation Network (CSN). (Fresh 2 vs. Aged 2 and Fresh 7 vs. Aged 7 represent the comparison of 2- and 7-days of atmospheric aging, respectively).

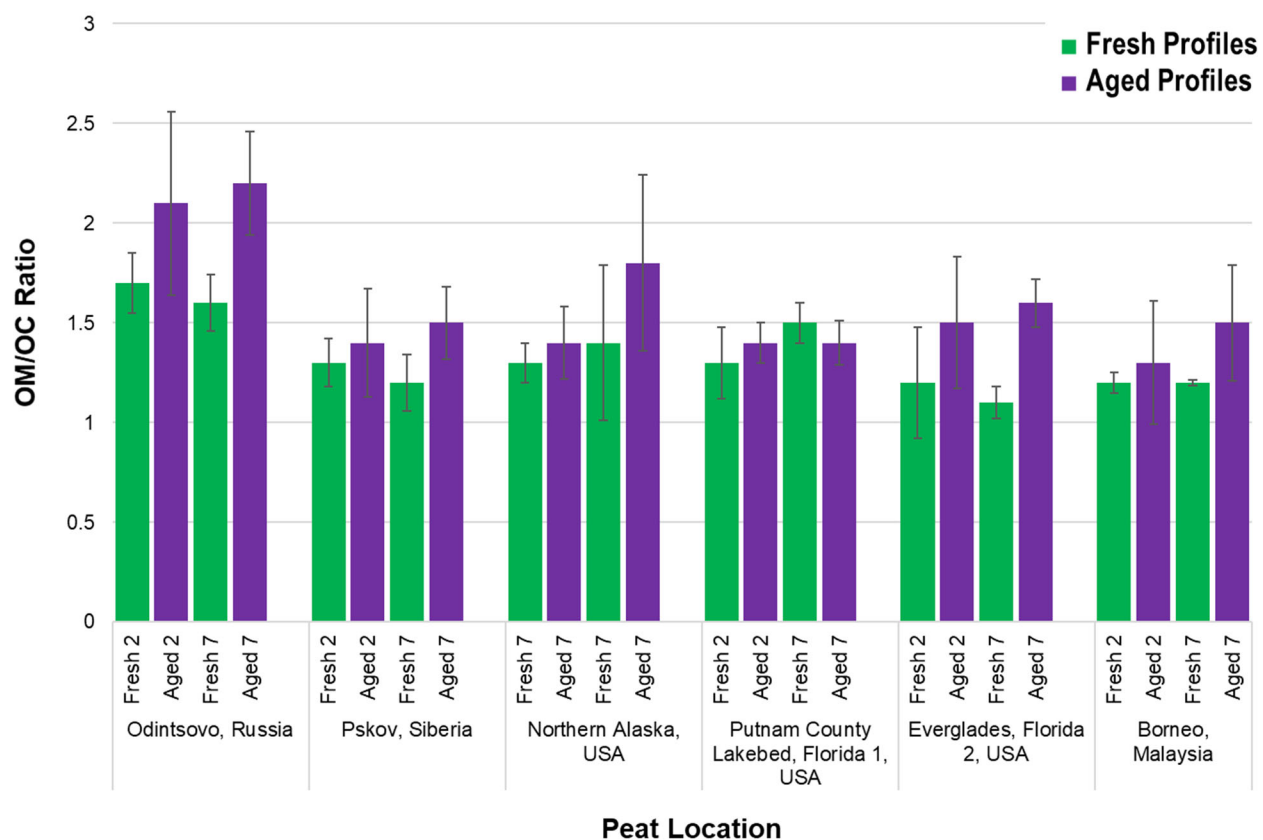


Figure S4. The OM/OC ratios between fresh and aged aerosol (Fresh 2 vs. Aged 2 and Fresh 7 vs. Aged 7 represent the comparison of 2- and 7-days of atmospheric aging, respectively).

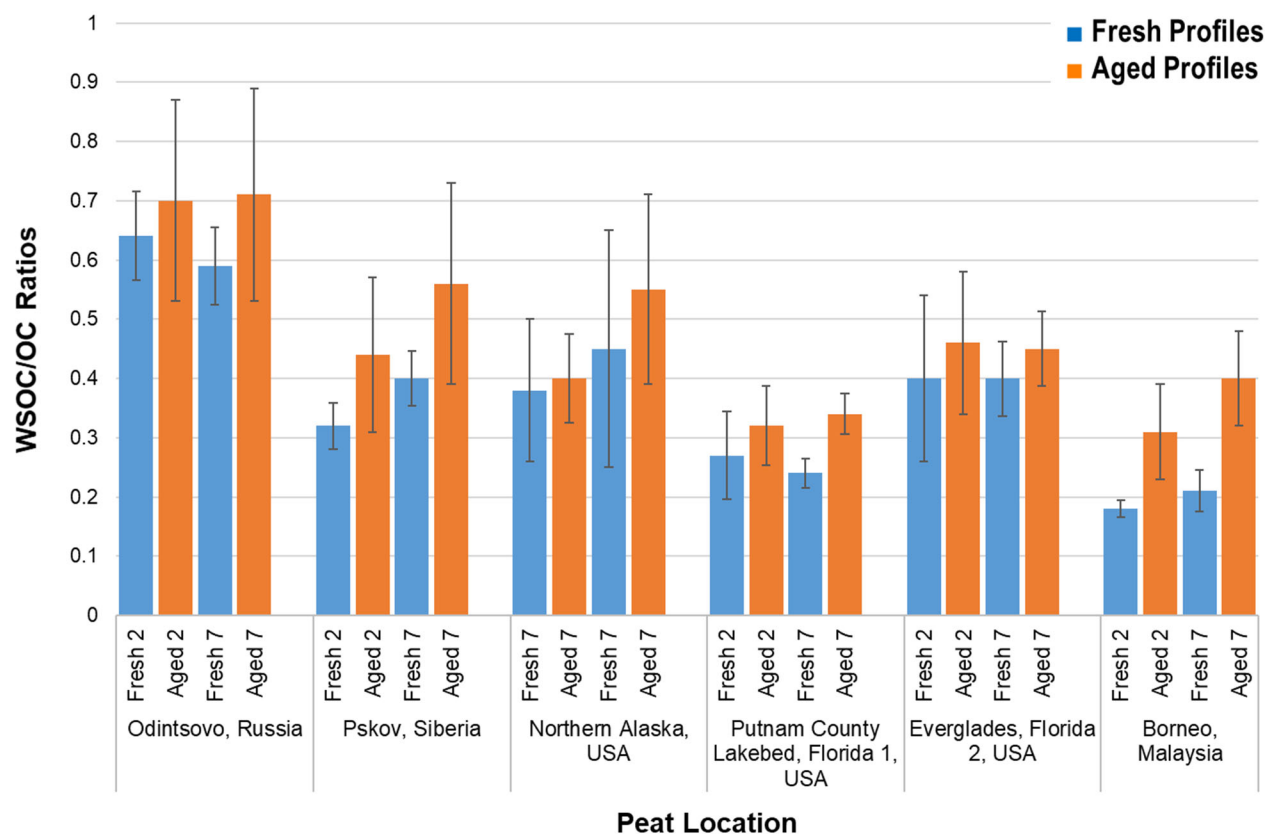


Figure S5. Ratios of water-soluble organic carbon (WSOC) OC between fresh and aged peat profiles (Fresh 2 vs. Aged 2 and Fresh 7 vs. Aged 7 represent the comparison of 2- and 7-days of atmospheric aging, respectively).

Table S1

Operational parameters for the 40 peat combustion tests

Peat Type	Peat ID	Voltage ^a (V)	Aging Time (days)	Reactor Relative Humidity (%)	Dilution Ratio	Modified Combustion Efficiency (MCE)	Peat Dry Mass before Burn (g)	Peat Dry Mass after Burn (g)	Sampling Duration (minutes)	Fresh Loading µg per filter	Aged Loading µg per filter	Ratio Aged/Fresh ± Std Dev	Fresh ^b PM _{2.5} Mass µg m ⁻³	Aged ^b PM _{2.5} Mass µg m ⁻³
Odintsovo, Russia	PEAT030	2	2	35	3.13	0.76	16.0	1.0	44	361.00	319.00	0.88 ± 0.019	1640.91	1450.00
	PEAT031	2	2	35	3.22	0.81	15.4	1.0	40	388.00	304.00	0.78 ± 0.017	1940.00	1520.00
	PEAT032	2	2	35	3.22	0.84	15.1	1.0	39	415.00	444.00	1.07 ± 0.018	2128.21	2276.92
	PEAT033	3.5	7	30	3.33	0.82	15.1	0.9	45	361.00	427.00	1.18 ± 0.022	1604.44	1897.78
	PEAT034	3.5	7	26	2.94	0.79	15.7	0.7	41	464.00	417.00	0.90 ± 0.015	2263.41	2034.15
	PEAT035	3.5	7	30	2.95	0.84	15.2	0.8	40	319.00	286.00	0.90 ± 0.022	1595.00	1430.00
Pskov, Siberia	PEAT023	2	2	20	5.03	0.84	47.1	1.9	67	558.00	557.00	1.00 ± 0.031	1665.67	1662.69
	PEAT025	2	2	55	4.71	0.85	25.8	1.0	70	NA ^d	257.00	NA ^d	NA ^d	734.29
	PEAT026	2	2	40	4.68	0.84	26.5	1.0	61	302.00	187.00	0.62 ± 0.0062	990.16	613.11
	PEAT027	3.5	7	40	4.68	0.87	25.6	1.0	52	206.00	142.00	0.69 ± 0.031	792.31	546.15
	PEAT028	3.5	7	50	4.72	0.83	25.7	1.1	57	384.00	411.00	1.07 ± 0.019	1347.37	1442.11
	PEAT029	3.5	7	35	4.74	0.85	26.1	1.1	68	256.00	304.00	1.19 ± 0.032	752.94	894.12
Northern Alaska, USA	PEAT013	2	2	30	4.78	0.84	58.2	13.2	95	246.00	NA ^d	NA ^d	517.89	NA ^d
	PEAT014	2	2	22	2.88	0.84	34.0	5.1	45	476.00	429.00	0.90 ± 0.014	2115.56	1906.67
	PEAT019	2	2	30	2.70	0.82	42.2	6.8	72	628.00	659.00	1.05 ± 0.012	1744.44	1830.56
	PEAT020	3.5	7	30	2.69	0.85	39.6	12.2	52	437.00	410.00	0.94 ± 0.016	1680.77	1576.92
	PEAT021 ^c	3.5	7	28	2.78	0.87	40.7	13.4	48	366.00	NA ^d	NA ^d	1525.00	NA ^d
	PEAT022	3.5	7	22	2.77	0.87	38.1	14.4	48	187.00	300.00	1.60 ± 0.053	779.17	1250.00
Putnam County Lakebed, Florida, USA (FL1)	PEAT007 ^e	2	2	40	5.02	0.57	41.7	2.5	84	NA ^d	NA ^d	NA ^d	NA ^d	NA ^d
	PEAT008	2	2	25	5.02	0.65	40.4	1.8	73	706.00	668.00	0.95 ± 0.010	1934.25	1830.14
	PEAT009	2	2	27	5.27	0.68	40.3	2.9	68	440.00	404.00	0.92 ± 0.017	1294.12	1188.24
	PEAT042 ^e	2	2	36	5.04	0.72	37.5	1.9	65	382.00	357.00	0.93 ± 0.019	1175.38	1098.46
	PEAT043 ^e	2	2	22	5.01	0.71	37.0	1.9	68	381.00	363.00	0.95 ± 0.019	1120.59	1067.65
	PEAT044 ^e	2	2	22	4.98	0.73	38.3	2.0	69	356.00	363.00	1.02 ± 0.021	1031.88	1052.17
	PEAT004 ^e	3.5	7	40	4.89	0.63	39.6	1.9	81	NA ^d	594.00	NA ^d	NA ^d	1466.67
	PEAT005	3.5	7	43	4.89	0.67	37.5	2.0	88	713.00	847.00	1.19 ± 0.011	1620.45	1925.00
Everglades National Park, Florida, USA (FL2)	PEAT006	3.5	7	44	4.90	0.58	38.3	2.5	91	648.00	657.00	1.01 ± 0.011	1424.18	1443.96
	PEAT010	2	2	25	5.13	0.91	41.3	13.9	111	182.00	340.00	1.87 ± 0.062	327.93	612.61
	PEAT011	2	2	25	4.10	0.90	61.2	21.5	135	545.00	487.00	0.89 ± 0.012	807.41	721.48
	PEAT012	2	2	17	4.09	0.95	66.5	29.1	119	262.00	247.00	0.94 ± 0.027	440.34	415.13
	PEAT015	2	2	30	3.97	0.87	31.8	11.0	55	227.00	223.00	0.98 ± 0.032	825.45	810.91
	PEAT016	3.5	7	33	4.21	0.90	64.7	31.1	85	232.00	410.00	1.77 ± 0.046	545.88	964.71
	PEAT017	3.5	7	48	4.03	0.88	64.2	16.1	113	496.00	971.00	1.96 ± 0.024	877.88	1718.58
	PEAT018	3.5	7	40	4.04	0.89	61.8	35.2	57	225.00	369.00	1.64 ± 0.044	789.47	1294.74
Borneo, Malaysia	PEAT036	2	2	37	2.97	0.87	30.3	9.3	66	406.00	322.00	0.79 ± 0.017	1230.30	975.76
	PEAT037 ^e	2	2	42	2.98	0.82	29.9	7.0	69	368.00	NA ^d	NA ^d	1066.67	NA ^d
	PEAT038	2	2	43	3.02	0.83	30.4	4.2	65	508.00	459.00	0.90 ± 0.014	1563.08	1412.31
	PEAT039	3.5	7	42	3.03	0.82	29.4	7.6	61	343.00	406.00	1.18 ± 0.024	1124.59	1331.15
	PEAT040 ^e	3.5	7	38	3.00	0.81	31.0	4.1	66	458.00	NA ^d	NA ^d	1387.88	NA ^d
	PEAT041	3.5	7	38	3.02	0.81	31.5	7.0	71	419.00	459.00	1.10 ± 0.019	1180.28	1292.96

^aUltraviolet lamp voltages (OFR185 mode) were used to simulate 2- and 7-days of atmospheric aging^bBased on 5 L min⁻¹ flow rate^cThese unpaired samples (fresh and aged, n=5) are not included in the averages by peat type^dData not available^eSamples are with 60 % fuel moisture (n=3) and are treated separately from others (25 % fuel moisture)

Table S2

Paired comparison of averaged fresh vs. aged peat combustion source profiles between 25% and 60% moisture content for Putnam County Lakebed, Florida (FL1) peat

Aging Time	Average \pm Standard Deviation of Percent PM _{2.5} Mass			
	Subtropical			
	Putnam County Lakebed, Florida (FL1)			
	2 days (25% fuel moisture)		2 days (60% fuel moisture)	
	Fresh 2	Aged 2	Fresh 2	Aged 2
Peat IDs in the average	PEAT008 and PEAT009		PEAT042, PEAT043, and PEAT044	
Nitric Acid (HNO ₃)	0.18 \pm 0.033	0.39 \pm 0.17	0.30 \pm 0.14	0.35 \pm 0.12
Ammonia (NH ₃)	28.030 \pm na	4.76 \pm 0.52	19.97 \pm 1.22	7.64 \pm 1.77
Water-Soluble Sodium (Na ⁺)	0.015 \pm 0.00033	4.060 \pm 5.70	0.020 \pm 0.0051	0.030 \pm 0.014
Water-Soluble Potassium (K ⁺)	0.010 \pm 0.015	na ^a	0.019 \pm 0.0074	na ^a
Chloride (Cl ⁻)	0.14 \pm 0.035	0.18 \pm 0.10	0.021 \pm 0.035	0.10 \pm 0.037
Nitrite (NO ₂ ⁻)	0.053 \pm 0.071	0.011 \pm 0.015	0.013 \pm 0.023	0.0012 \pm 0.0013
Nitrate (NO ₃ ⁻)	0.16 \pm 0.12	0.87 \pm 0.15	0.13 \pm 0.093	0.48 \pm 0.12
Sulfate (SO ₄ ⁼)	0.89 \pm 0.97	1.60 \pm 1.33	0.17 \pm 0.031	0.74 \pm 0.032
Ammonium (NH ₄ ⁺)	0.00070 \pm 0.00099	0.052 \pm 0.074	0.0028 \pm 0.0012	0.39 \pm 0.049
OC1 (140 °C)	9.54 \pm 2.50	7.48 \pm 3.12	11.93 \pm 3.51	5.25 \pm 0.79
OC2 (280 °C)	21.66 \pm 2.045	19.50 \pm 0.85	20.98 \pm 0.40	15.66 \pm 2.71
OC3 (480 °C)	25.30 \pm 7.61	24.97 \pm 0.95	29.42 \pm 1.63	25.93 \pm 3.050
OC4 (580 °C)	7.60 \pm 4.045	7.76 \pm 1.017	6.71 \pm 1.35	7.61 \pm 2.46
Pyrolyzed Carbon	7.61 \pm 1.80	10.45 \pm 1.14	12.90 \pm 0.72	9.59 \pm 2.18
Organic Carbon (OC) ^b	71.71 \pm 9.40	70.16 \pm 5.033	81.94 \pm 3.86	64.032 \pm 7.51
EC1 (580 °C)	7.61 \pm 2.43	9.58 \pm 1.36	9.33 \pm 0.85	8.19 \pm 1.15
EC2 (740 °C)	3.51 \pm 2.51	2.94 \pm 2.34	6.38 \pm 0.055	3.81 \pm 1.010
EC3 (840 °C)	0.00 \pm 0.00	0.00 \pm 0.00	0.00 \pm 0.00	0.00 \pm 0.00
Elemental Carbon (EC) ^b	3.51 \pm 1.72	2.076 \pm 0.16	2.80 \pm 0.42	2.42 \pm 2.43
Total Carbon (TC)	75.23 \pm 11.12	72.24 \pm 4.88	84.74 \pm 4.26	66.45 \pm 9.51
Water-Soluble OC (WSOC)	19.53 \pm 4.67	22.71 \pm 4.43	29.61 \pm 14.67	23.75 \pm 4.02
Formic acid (CH ₂ O ₂)	0.11 \pm 0.097	0.20 \pm 0.13	0.13 \pm 0.049	0.27 \pm 0.053
Acetic acid (C ₂ H ₄ O ₂)	0.19 \pm 0.15	0.047 \pm 0.011	0.57 \pm 0.22	0.78 \pm 0.34
Oxalic acid (C ₂ H ₂ O ₄)	0.050 \pm 0.070	0.58 \pm 0.26	0.38 \pm 0.091	0.73 \pm 0.070
Propionic acid (C ₃ H ₆ O ₂)	0.00 \pm 0.00	0.00 \pm 0.00	0.021 \pm 0.019	0.021 \pm 0.036
Levogluconan (C ₆ H ₁₀ O ₅)	3.15 \pm 0.0092	2.78 \pm 0.041	3.79 \pm 0.42	2.45 \pm 0.22
Mannosan (C ₆ H ₁₀ O ₅)	0.00 \pm 0.00	0.00 \pm 0.00	0.25 \pm 0.42	0.29 \pm 0.50
Galactose/Maltitol (C ₆ H ₁₂ O ₆ /C ₁₂ H ₂₄ O ₁₁)	0.00 \pm 0.00	0.00 \pm 0.00	0.00 \pm 0.00	0.00 \pm 0.00
Glycerol (C ₃ H ₈ O ₃)	0.00 \pm 0.00	0.00 \pm 0.00	0.096 \pm 0.11	0.00 \pm 0.00
Mannitol (C ₆ H ₁₄ O ₆)	0.00 \pm 0.00	0.00 \pm 0.00	0.00 \pm 0.00	0.00 \pm 0.00
Aluminum (Al)	0.026 \pm 0.059	0.069 \pm 0.97	0.043 \pm 0.49	0.13 \pm 0.16
Silicon (Si)	0.00 \pm 0.00	0.021 \pm 0.22	0.018 \pm 0.30	0.14 \pm 0.45
Phosphorous (P)	0.00 \pm 0.00	0.00 \pm 0.00	0.00 \pm 0.00	0.00 \pm 0.00

Table S2 (cont'd)

Aging Time	Average \pm Standard Deviation of Percent PM _{2.5} Mass			
	Subtropical			
	Putnam County Lakebed, Florida (FL1)			
	2 days (25% fuel moisture)		2 days (60% fuel moisture)	
	Fresh 2	Aged 2	Fresh 2	Aged 2
Peat IDs in the average	PEAT008 and PEAT009		PEAT042, PEAT043, and PEAT044	
Sulfur (S)	0.19 \pm 0.056	0.37 \pm 0.24	0.13 \pm 0.021	0.54 \pm 0.019
Chlorine (Cl)	0.12 \pm 0.0064	0.067 \pm 0.024	0.18 \pm 0.028	0.079 \pm 0.0082
Potassium (K)	0.0092 \pm 0.012	0.057 \pm 0.035	0.22 \pm 0.016	0.028 \pm 0.0080
Calcium (Ca)	0.0040 \pm 0.0056	0.00 \pm 0.00	0.013 \pm 0.023	0.00 \pm 0.00
Scandium (Sc)	0.00 \pm 0.00	0.00 \pm 0.00	0.00 \pm 0.00	0.00 \pm 0.00
Titanium (Ti)	0.0036 \pm 0.0050	0.00 \pm 0.00	0.00 \pm 0.00	0.00 \pm 0.00
Vanadium (V)	0.00 \pm 0.00	0.00 \pm 0.00	0.00 \pm 0.00	0.00 \pm 0.00
Chromium (Cr)	0.00 \pm 0.00	0.00 \pm 0.00	0.0011 \pm 0.0016	0.016 \pm 0.023
Manganese (Mn)	0.0013 \pm 0.0012	0.00033 \pm 0.00047	0.0065 \pm 0.0026	0.00077 \pm 0.0011
Iron (Fe)	0.00 \pm 0.00	0.047 \pm 0.040	0.038 \pm 0.012	0.13 \pm 0.12
Cobalt (Co)	0.00 \pm 0.00	0.00021 \pm 0.00030	0.00 \pm 0.00	0.00 \pm 0.00
Nickel (Ni)	0.00045 \pm 0.00064	0.00 \pm 0.00	0.00 \pm 0.00	0.00 \pm 0.00
Copper (Cu)	0.00 \pm 0.00	0.0035 \pm 0.0049	0.036 \pm 0.033	0.027 \pm 0.024
Zinc (Zn)	0.0013 \pm 0.0015	0.0023 \pm 0.0032	0.025 \pm 0.021	0.026 \pm 0.026
Arsenic (As)	0.00 \pm 0.00	0.00 \pm 0.00	0.00 \pm 0.00	0.00 \pm 0.00
Selenium (Se)	0.0017 \pm 0.00092	0.00 \pm 0.00	0.0020 \pm 0.0024	0.0033 \pm 0.0047
Bromine (Br)	0.020 \pm 0.00098	0.0077 \pm 0.010	0.022 \pm 0.0065	0.013 \pm 0.0024
Rubidium (Rb)	0.00011 \pm 0.00016	0.00095 \pm 0.0013	0.0012 \pm 0.0018	0.0019 \pm 0.0026
Strontium (Sr)	0.0023 \pm 0.00057	0.0038 \pm 0.0013	0.0061 \pm 0.0019	0.0042 \pm 0.0026
Yttrium (Y)	0.0014 \pm 0.00029	0.0012 \pm 0.0018	0.0030 \pm 0.0041	0.0029 \pm 0.0017
Zirconium (Zr)	0.0016 \pm 0.0023	0.0003 \pm 0.00089	0.0042 \pm 0.0046	0.0070 \pm 0.0038
Niobium (Nb)	0.0016 \pm 0.0023	0.00082 \pm 0.0012	0.0013 \pm 0.0015	0.0013 \pm 0.0019
Molybdenum (Mo)	0.00 \pm 0.00	0.00063 \pm 0.00089	0.0034 \pm 0.0036	0.0013 \pm 0.0019
Silver (Ag)	0.0010 \pm 0.0014	0.00 \pm 0.00	0.00 \pm 0.00	0.00 \pm 0.00
Cadmium (Cd)	0.0034 \pm 0.0049	0.00 \pm 0.00	0.00 \pm 0.00	0.00 \pm 0.00
Indium (In)	0.00068 \pm 0.00096	0.0025 \pm 0.0036	0.0025 \pm 0.0024	0.0038 \pm 0.0054
Tin (Sn)	0.0037 \pm 0.00047	0.0034 \pm 0.0048	0.00049 \pm 0.00085	0.0066 \pm 0.0093
Antimony (Sb)	0.00 \pm 0.00	0.0072 \pm 0.010	0.0031 \pm 0.0053	0.010 \pm 0.014
Cesium (Cs)	0.00 \pm 0.00	0.00 \pm 0.00	0.018 \pm 0.029	0.0086 \pm 0.012
Barium (Ba)	0.00 \pm 0.00	0.00 \pm 0.00	0.013 \pm 0.022	0.00 \pm 0.00
Lanthanum (La)	0.042 \pm 0.044	0.0053 \pm 0.0075	0.045 \pm 0.039	0.010 \pm 0.014
Wolfram (W)	0.0037 \pm 0.0018	0.0034 \pm 0.0049	0.00010 \pm 0.00018	0.0053 \pm 0.0075
Gold (Au)	0.00062 \pm 0.00088	0.00 \pm 0.00	0.0016 \pm 0.0015	0.00 \pm 0.00
Mercury (Hg)	0.00020 \pm 0.00028	0.0014 \pm 0.0020	0.00 \pm 0.00	0.00 \pm 0.00
Lead (Pb)	0.0015 \pm 0.0021	0.0014 \pm 0.000962	0.0038 \pm 0.0063	0.0033 \pm 0.00
Uranium (U)	0.0034 \pm 0.0044	0.00 \pm 0.00	0.0023 \pm 0.0040	0.0036 \pm 0.0051

^aWater-soluble K⁺ data were contaminated due to the use of potassium iodide denuder downstream of the oxidation flow reactor

^bThe carbon analysis follows the IMPROVE_A thermal/optical reflectance protocol (Chow et al., 2007) that is applied in long-term U.S. non-urban IMPROVE and urban Chemical Speciation Network. Organic carbon (OC) is the sum of OC1+OC2+OC3+OC4 plus pyrolyzed carbon (OP). Elemental carbon (EC) is the sum of EC1+EC2+EC3 minus OP. Total carbon is the sum of OC and EC. Since a large fraction of OP (7–13 %) are found in smoldering peat combustion emissions--indicative of higher molecular-weight compounds that are likely to char, the resulting EC are lower than the individual EC fraction after OP correction.

Table S3
Unpaired fresh or aged peat source profiles

	Average ± Standard Deviation of Percent PM _{2.5} Mass				
Peat Location	Pskov, Siberia	Northern Alaska, USA	Putnam County Lakebed, Florida (FL1), USA	Borneo, Malaysia	Borneo, Malaysia
Aging Time	Fresh 2	Fresh 7	Aged 7	Fresh 2	Fresh 7
Peat ID	PEAT024	PEAT021	PEAT004	PEAT037	PEAT040- F7
Nitric Acid (HNO ₃)	0.25 ± 0.00026	0.22 ± 0.00019	0.39 ± 0.00019	0.21 ± 0.00019	0.28 ± 0.00018
Ammonia (NH ₃)	20.50 ± 0.0071	8.86 ± 0.0028	1.84 ± 0.00055	25.088 ± 0.0080	22.63 ± 0.0069
Water-Soluble Sodium (Na ⁺)	0.025 ± 0.00083	0.032 ± 0.00060	0.046 ± 0.00037	0.013 ± 0.00060	0.012 ± 0.00048
Water-Soluble Potassium (K ⁺)	0.051 ± 0.000083	0.035 ± 0.000059	na ^a	0.027 ± 0.000056	0.036 ± 0.000051
Chloride (Cl ⁻)	0.16 ± 0.00024	0.21 ± 0.00019	0.10 ± 0.00011	0.10 ± 0.00017	0.12 ± 0.00014
Nitrite (NO ₂ ⁻)	0.00 ± 0.00040	0.00 ± 0.00029	0.0011 ± 0.00018	0.00 ± 0.00029	0.0055 ± 0.00023
Nitrate (NO ₃ ⁻)	0.087 ± 0.00048	0.097 ± 0.00035	2.038 ± 0.00099	0.080 ± 0.00034	0.075 ± 0.00028
Sulfate (SO ₄ ⁼)	0.63 ± 0.00044	0.19 ± 0.00014	1.78 ± 0.0012	0.25 ± 0.00018	0.17 ± 0.00012
Ammonium (NH ₄ ⁺)	0.0024 ± 0.00012	0.0017 ± 0.000086	1.60 ± 0.0012	0.0017 ± 0.000086	0.0021 ± 0.000069
OC1 (140°C)	11.36 ± 0.028	15.22 ± 0.038	8.61 ± 0.021	11.26 ± 0.028	12.92 ± 0.032
OC2 (280°C)	20.84 ± 0.013	15.56 ± 0.0094	21.65 ± 0.012	24.48 ± 0.014	24.47 ± 0.014
OC3 (480°C)	28.60 ± 0.022	24.19 ± 0.018	27.92 ± 0.021	29.83 ± 0.022	27.041 ± 0.020
OC4 (590°C)	9.29 ± 0.0083	4.27 ± 0.0038	6.75 ± 0.0059	9.17 ± 0.0081	8.090 ± 0.0071
Pyrolyzed Carbon	13.04 ± 0.021	12.18 ± 0.019	11.58 ± 0.018	9.71 ± 0.015	8.90 ± 0.014
Organic Carbon (OC) ^c	83.13 ± 0.046	71.42 ± 0.038	76.52 ± 0.040	84.45 ± 0.045	81.41 ± 0.043
EC1 (580°C)	6.47 ± 0.014	7.043 ± 0.016	12.061 ± 0.026	7.11 ± 0.016	6.14 ± 0.014
EC2 (740°C)	6.95 ± 0.0077	5.13 ± 0.0056	2.15 ± 0.0024	4.17 ± 0.0046	4.88 ± 0.0053
EC3 (840°C)	0.00 ± 0.00028	0.00 ± 0.00021	0.00 ± 0.00013	0.00 ± 0.00020	0.00 ± 0.00016
Elemental Carbon (EC) ^c	0.38 ± 0.0017	0.00 ± 0.0011	2.63 ± 0.0038	1.56 ± 0.0025	2.12 ± 0.0031
Total Carbon (TC)	83.51 ± 0.044	71.42 ± 0.036	79.15 ± 0.039	86.012 ± 0.043	83.54 ± 0.041
Water-Soluble OC	28.17 ± 0.038	31.49 ± 0.042	26.04 ± 0.035	17.14 ± 0.023	15.90 ± 0.021
Formic acid (CH ₂ O ₂)	0.047 ± 0.000069	0.074 ± 0.00011	0.19 ± 0.00028	0.14 ± 0.00021	0.11 ± 0.00016
Acetic acid (C ₂ H ₄ O ₂)	0.28 ± 0.00034	0.41 ± 0.00049	0.25 ± 0.00030	0.47 ± 0.00057	0.32 ± 0.00039
Oxalic acid (C ₂ H ₂ O ₄)	0.00 ± 0.00	0.00 ± 0.00	1.45 ± 0.0022	0.27 ± 0.00041	0.33 ± 0.00049
Propionic acid (C ₃ H ₆ O ₂)	0.050 ± 0.00020	0.00 ± 0.00014	0.00 ± 0.000088	0.00 ± 0.00014	0.020 ± 0.00011
Levogluconan (C ₆ H ₁₀ O ₅)	6.17 ± 0.015	11.82 ± 0.029	2.40 ± 0.0059	4.084 ± 0.010	5.66 ± 0.014
Mannosan (C ₆ H ₁₀ O ₅)	0.00 ± 0.00043	5.32 ± 0.016	0.00 ± 0.00019	0.00 ± 0.00031	1.27 ± 0.0081
Galactose/Maltitol (C ₆ H ₁₂ O ₆ /C ₁₂ H ₂₄ O ₁₁)	0.00 ± 0.00022	0.00 ± 0.00016	0.00 ± 0.000099	0.00 ± 0.00016	0.00 ± 0.00013
Glycerol (C ₃ H ₈ O ₃)	0.00 ± 0.0000040	0.00 ± 0.0000029	0.00 ± 0.0000018	0.00 ± 0.0000029	0.00 ± 0.0000023
Mannitol (C ₆ H ₁₄ O ₆)	0.00 ± 0.000079	0.00 ± 0.000057	0.00 ± 0.000035	0.00 ± 0.000057	0.00 ± 0.000046
Aluminum (Al)	0.00 ± 0.052	0.053 ± 0.038	na ^b	0.074 ± 0.038	0.016 ± 0.030
Silicon (Si)	0.00 ± 0.0061	0.043 ± 0.0045	na ^b	0.0071 ± 0.0045	0.0023 ± 0.0036
Phosphorous (P)	0.00 ± 0.00012	0.00 ± 0.000089	na ^b	0.00 ± 0.000088	0.00 ± 0.000071

Table S3 (cont'd)

	Average \pm Standard Deviation of Percent PM _{2.5} Mass				
Peat Location	Pskov, Siberia	Northern Alaska, USA	Putnam County Lakebed, Florida (FL1), USA	Borneo, Malaysia	Borneo, Malaysia
Aging Time	Fresh 2	Fresh 7	Aged 7	Fresh 2	Fresh 7
Peat ID	PEAT024	PEAT021	PEAT004	PEAT037	PEAT040- F7
Sulfur (S)	0.00 \pm 0.000065	0.094 \pm 0.000058	na ^b	0.097 \pm 0.000058	0.091 \pm 0.000048
Chlorine (Cl)	0.12 \pm 0.000064	0.15 \pm 0.000060	na ^b	0.082 \pm 0.000043	0.12 \pm 0.000046
Potassium (K)	0.047 \pm 0.00017	0.11 \pm 0.00013	na ^b	0.026 \pm 0.00013	0.027 \pm 0.00010
Calcium (Ca)	0.00 \pm 0.00065	0.010 \pm 0.00047	na ^b	0.00 \pm 0.00046	0.00 \pm 0.00037
Scandium (Sc)	0.00 \pm 0.0029	0.00 \pm 0.0021	na ^b	0.00 \pm 0.0021	0.00 \pm 0.0017
Titanium (Ti)	0.00 \pm 0.00010	0.030 \pm 0.000075	na ^b	0.016 \pm 0.000074	0.013 \pm 0.000060
Vanadium (V)	0.00 \pm 0.000019	0.00 \pm 0.000014	na ^b	0.00 \pm 0.000014	0.00 \pm 0.000011
Chromium (Cr)	0.00 \pm 0.000065	0.025 \pm 0.000047	na ^b	0.00 \pm 0.000046	0.00 \pm 0.000037
Manganese (Mn)	0.00 \pm 0.00023	0.015 \pm 0.00016	na ^b	0.012 \pm 0.00016	0.0083 \pm 0.00013
Iron (Fe)	0.00 \pm 0.00039	0.24 \pm 0.00030	na ^b	0.041 \pm 0.00028	0.014 \pm 0.00023
Cobalt (Co)	0.00 \pm 0.000013	0.00 \pm 0.0000093	na ^b	0.00010 \pm 0.0000092	0.00 \pm 0.0000074
Nickel (Ni)	0.0006 \pm 0.000032	0.0070 \pm 0.000023	na ^b	0.00010 \pm 0.000023	0.00030 \pm 0.000019
Copper (Cu)	0.00 \pm 0.00020	0.0051 \pm 0.00015	na ^b	0.00 \pm 0.00014	0.0035 \pm 0.00012
Zinc (Zn)	0.0024 \pm 0.00011	0.0054 \pm 0.000079	na ^b	0.0021 \pm 0.000079	0.0077 \pm 0.000063
Arsenic (As)	0.0031 \pm 0.000051	0.00 \pm 0.000037	na ^b	0.00 \pm 0.000037	0.00 \pm 0.000030
Selenium (Se)	0.0014 \pm 0.000090	0.00 \pm 0.000065	na ^b	0.00 \pm 0.000065	0.00 \pm 0.000052
Bromine (Br)	0.0036 \pm 0.000026	0.0030 \pm 0.000019	na ^b	0.013 \pm 0.000019	0.0089 \pm 0.000015
Rubidium (Rb)	0.00 \pm 0.000032	0.00 \pm 0.000023	na ^b	0.00080 \pm 0.000023	0.0014 \pm 0.000019
Strontium (Sr)	0.0041 \pm 0.000032	0.0036 \pm 0.000023	na ^b	0.0049 \pm 0.000023	0.0045 \pm 0.000019
Yttrium (Y)	0.00 \pm 0.000032	0.0083 \pm 0.000023	na ^b	0.00 \pm 0.000023	0.00010 \pm 0.000019
Zirconium (Zr)	0.0041 \pm 0.00012	0.0020 \pm 0.000089	na ^b	0.0062 \pm 0.000088	0.0040 \pm 0.000071
Niobium (Nb)	0.00 \pm 0.000058	0.00 \pm 0.000042	na ^b	0.00 \pm 0.000042	0.00030 \pm 0.000034
Molybdenum (Mo)	0.0027 \pm 0.00012	0.00 \pm 0.000089	na ^b	0.00 \pm 0.000088	0.0010 \pm 0.000071
Silver (Ag)	0.00 \pm 0.00015	0.00 \pm 0.00011	na ^b	0.00 \pm 0.00011	0.00 \pm 0.000089
Cadmium (Cd)	0.00 \pm 0.00021	0.00 \pm 0.00015	na ^b	0.00 \pm 0.00015	0.00 \pm 0.00012
Indium (In)	0.015 \pm 0.00015	0.00 \pm 0.00011	na ^b	0.00 \pm 0.00011	0.0026 \pm 0.000086
Tin (Sn)	0.0021 \pm 0.00027	0.00 \pm 0.00020	na ^b	0.018 \pm 0.00019	0.011 \pm 0.00016
Antimony (Sb)	0.00 \pm 0.00041	0.00 \pm 0.00029	na ^b	0.00 \pm 0.00029	0.0061 \pm 0.00023
Cesium (Cs)	0.00 \pm 0.0011	0.00 \pm 0.00082	na ^b	0.045 \pm 0.00082	0.00 \pm 0.00066
Barium (Ba)	0.00 \pm 0.00085	0.00 \pm 0.00062	na ^b	0.00 \pm 0.00061	0.00 \pm 0.00049
Lanthanum (La)	0.16 \pm 0.0017	0.00 \pm 0.0012	na ^b	0.00 \pm 0.0012	0.00 \pm 0.00097
Wolfram (W)	0.00 \pm 0.00033	0.0056 \pm 0.00024	na ^b	0.00 \pm 0.00024	0.016 \pm 0.00019
Gold (Au)	0.0011 \pm 0.000097	0.00 \pm 0.000070	na ^b	0.00 \pm 0.000070	0.00 \pm 0.000056
Mercury (Hg)	0.00 \pm 0.000051	0.00 \pm 0.000037	na ^b	0.00 \pm 0.000037	0.00 \pm 0.000030
Lead (Pb)	0.00 \pm 0.000097	0.00 \pm 0.000070	na ^b	0.00 \pm 0.000070	0.00 \pm 0.000056
Uranium (U)	0.017 \pm 0.00017	0.0038 \pm 0.00013	na ^b	0.0012 \pm 0.00013	0.0044 \pm 0.00010

^aWater-soluble K⁺ data were contaminated due to the use of potassium iodide denuder downstream of the oxidation flow reactor

^bData not available due to the lack of elemental measurements from x-ray fluorescence analysis

^cThe carbon analysis follows the IMPROVE_A thermal/optical reflectance protocol (Chow et al., 2007) that is applied in long-term U.S. non-urban IMPROVE and urban Chemical Speciation Network. Organic carbon (OC) is the sum of OC1+OC2+OC3+OC4 plus pyrolyzed carbon (OP). Elemental carbon (EC) is the sum of EC1+EC2+EC3 minus OP. Total carbon is the sum of OC and EC. Since a large fraction of OP (7–13 %) are found in smoldering peat combustion emissions--indicative of higher molecular-weight compounds that are likely to char, the resulting EC are lower than the individual EC fraction after OP correction.

Table S4

Equivalence measures^a for paired fresh and aged source profiles for the Putnam County Lakebed (FL1) and Everglades National Park (FL2), Florida peats.

A. Putnam County Lakebed (FL1) vs. Everglades National Park (FL2)								
Paired Comparison ^b	R/U Ratio Percent Distribution				Correlation Coefficient (r)	Student <i>t</i> -Test	df ^c	<i>P</i> -value
	< 1 σ	1 - 2 σ	2 - 3 σ	> 3 σ				
FL1 Fresh 2 vs. FL2 Fresh 2	82.26%	16.13%	0.81%	0.81%	0.996	Paired	126	0.0000
FL1 Fresh 7 vs. FL2 Fresh 7	59.20%	18.40%	16.80%	5.60%	0.998	Paired	126	0.0000
FL1 Aged 2 vs. FL2 Aged 2	92.00%	6.40%	0.80%	0.80%	0.998	Paired	126	0.0006
FL1 Aged 7 vs. FL2 Aged 7	60.32%	15.87%	17.46%	6.35%	0.994	Paired	126	0.0015

B. FL1 and FL2 combined								
Paired Comparison ^d	R/U Ratio Percent Distribution				Correlation Coefficient (r)	Student <i>t</i> -Test	df ^c	<i>P</i> -value
	< 1 σ	1 - 2 σ	2 - 3 σ	$\geq 3 \sigma$				
All Fresh 2 vs. All Aged 2	92.86%	6.35%	0.79%	0.00%	0.992	Paired	126	0.0000
All Fresh 7 vs. All Aged 7	73.02%	23.81%	2.38%	0.79%	0.974	Paired	126	0.0002
All Fresh 2 vs. All Fresh 7	98.41%	1.59%	0.00%	0.00%	0.997	Paired	126	0.5234
All Aged 2 vs. All Aged 7	93.65%	6.35%	0.00%	0.00%	0.998	Paired	126	0.0019
All Fresh vs. All Aged	92.86%	7.14%	0.00%	0.00%	0.985	Paired	126	0.0001

^aFor the *t*-test, a cutoff probability level of 5% is selected; if $P < 0.05$, there is a 95% probability that the two profiles are different. For correlations, $r > 0.8$ suggests similar profiles, $0.5 < r < 0.8$ indicates a moderate similarity, and $r < 0.5$ denotes little or no similarity. The *R/U* ratio indicates the percentage of the >93 reported chemical abundances differ by more than an expected number of uncertainty intervals. The normal probability density function of 68%, 95.5%, and 99.7% for $\pm 1 \sigma$, $\pm 2 \sigma$, and $\pm 3 \sigma$, respectively, is used to evaluate the *R/U* ratios. The two profiles are considered to be similar, within the uncertainties of the chemical abundances when 80% of the *R/U* ratios are within $\pm 3 \sigma$, with $r > 0.8$ and $P > 0.05$. Species with *R/U* ratios $> 3 \sigma$ are further examined as these may be markers that further allow source contributions to be distinguished by receptor measurements. They may also reflect the sampling and analysis artifacts that are not representative of the larger population of source profiles.

^bIncludes two paired samples for 2- and 7-days of atmospheric aging.

^cDegree of freedom

^d"All Fresh 2" includes fresh, unaged profiles from both Putnam (FL1) and Everglades (FL2) peats for the 2-days experiment (same as "All Fresh 7" for the 7-days experiment); "All Aged 2" includes 2-day aged profiles from both Putnam (FL1) and Everglades (FL2) peats, downstream of the oxidation flow reactor for the 2-days aging experiment (same as "All Aged 7" for the 7-days aging experiment); "All Fresh" includes combined Putnam (FL1) and Everglades (FL2) Fresh 2 and Fresh 7 peats (same as "All Aged" for Aged 2 and Aged 7 peats).

Table S5

Summary of Student *t*-tests for fresh vs. aged peat combustion source profiles for PM_{2.5} mass ($\mu\text{g m}^{-3}$).

Paired Comparison	n1 ^a	n2 ^a	Student <i>t</i> -Test	df ^b	<i>P</i> -value ^c
All Fresh vs. All Aged ^d	32	32	paired	31	0.504
Fresh2 vs. Aged2	17	17	paired	16	0.043
Fresh7 vs. Aged7	15	15	paired	14	0.041
Fresh2 vs. Fresh7	17	15	2 sample	30	0.712
Aged2 vs. Aged7	17	15	2 sample	30	0.272

^aIncludes 17 and 15 paired fresh and aged profiles for 2- and 7-days of atmospheric aging, respectively.

^bDegree of freedom

^cStudent *t*-tests, a cutoff probability level of 5% is selected. The highlighted *P*-value denotes that $P < 0.05$ and there is a 95% probability that two profiles are different.

^d"All Fresh" includes both Fresh 2 and Fresh 7 profiles; and "All Aged" includes both Aged 2 and Aged 7 profiles.

Table S6

Percent (%) of PM_{2.5} mass explained by the sum of measured species for the six peats

Type of Peat	(Sum of Species ^a /Mass) x 100%			
	Fresh 2	Aged 2	Fresh 7	Aged 7
Odintsovo, Russia	62.2 ± 1.8	52.3 ± 6.1	63.5 ± 5.0	50.2 ± 7.7
Pskov, Siberia	79.1 ± 5.6	75.9 ± 13.4	83.7 ± 10.4	72.8 ± 13.4
Northern Alaska, USA	82.8 ± 6.5	76.7 ± 9.3	75.5 ± 21.3	63.3 ± 5.3
Putnam County Lakebed, Florida, USA (FL1)	80.3 ± 17.5	79.3 ± 2.5	69.8 ± 4.7	73.4 ± 5.0
Everglades National Park, Florida, USA (FL2)	89.8 ± 28.1	73.0 ± 10.1	88.4 ± 7.2	69.0 ± 4.4
Borneo, Malaysia	80.9 ± 3.6	79.5 ± 18.8	83.1 ± 1.3	70.2 ± 9.0
Average ± SD	79.2 ± 10.5	72.8 ± 10.0	77.3 ± 8.3	66.5 ± 7.5

^aSum of species includes 51 elements, water-soluble Na⁺, NH₄⁺, NO₂⁻, NO₃⁻, SO₄²⁻, OC, and EC. Water-soluble Cl⁻ and K⁺ by ion chromatography are not included because of the inclusion of Cl and K measured by x-ray fluorescence, to avoid double counting.

Table S7

Differences of WSOC abundances^a in PM_{2.5} between the aged and fresh profiles

Peat Location	Differences and associated uncertainties between aged and fresh WSOC abundances in PM _{2.5}	
	2-day aging	7-day aging
Odintsovo, Russia	-5.17 ± 4.16 ^b	-6.56 ± 6.72
Pskov, Siberia	6.04 ± 7.34	-2.62 ± 8.91
Northern Alaska, USA	-0.97 ± 9.80	-5.81 ± 11.93
Putnam County Lakebed, USA (FL1)	3.18 ± 6.44	6.82 ± 1.86
Everglades National Park, USA (FL2)	-2.82 ± 9.30	-11.05 ± 5.57
Borneo, Malaysia	8.26 ± 2.51	5.75 ± 2.90

^aSee Table 1 for WSOC (water-soluble organic carbon) abundances in PM_{2.5}.^bDifference in WSOC abundance= Aged minus Fresh. Plus or minus signs indicate the increase and decrease, respectively in WSOC/PM_{2.5} ratios after atmospheric aging; the uncertainty of the difference is based on square root of the sum of the squared uncertainties associated with each averaged profile.

Table S8

Equivalence measures^a for 25 and 60% fuel moisture content source profiles for the Putnam County Lakebed, Florida (FL1) peat.

Paired Comparison ^b	Percent Distribution				Correlation Coefficient (r)	Student <i>t</i> -Test	df ^c	<i>P</i> -value
	< 1 σ	1 - 2 σ	2 - 3 σ	$\geq 3 \sigma$				
FL25 Fresh2 vs. FL60 Fresh2	73.39%	16.13%	4.03%	6.45%	0.997	Paired	126	0.00000021
FL25 Aged2 vs. FL60 Aged2	88.80%	6.40%	2.40%	2.40%	0.999	Paired	126	0.00020671
All Fresh vs. All Aged	79.37%	19.84%	0.00%	0.79%	0.998	Paired	126	0.00000243

^aFor the *t*-test, a cutoff probability level of 5% is selected; if $P < 0.05$, there is a 95% probability that the two profiles are different. For correlations, $r > 0.8$ suggests similar profiles, $0.5 < r < 0.8$ indicates a moderate similarity, and $r < 0.5$ denotes little or no similarity. The *R/U* ratio indicates the percentage of the >93 reported chemical abundances differ by more than an expected number of uncertainty intervals. The normal probability density function of 68%, 95.5%, and 99.7% for $\pm 1\sigma$, $\pm 2\sigma$, and $\pm 3\sigma$, respectively, is used to evaluate the *R/U* ratios. The two profiles are considered to be similar, within the uncertainties of the chemical abundances when 80% of the *R/U* ratios are within $\pm 3\sigma$ with $r > 0.8$ and $P > 0.05$. Species with *R/U* ratios $> 3\sigma$ are further examined as these may be markers that further allow source contributions to be distinguished by receptor measurements. They may also reflect the sampling and analysis artifacts that are not representative of the larger population of source profiles.

^bFL25 and FL60 denote peats with 25% and 60% fuel moisture contents; "All Fresh" and "All Aged" includes both 25% and 60% fuel moisture content peats for the Fresh vs. Aged comparison with 2-day aging times.

^cDegree of freedom